Dispersion-Independent High-Visibility Quantum Interference in Ultrafast Parametric Down-Conversion

Mete Atatüre,[1] Alexander V. Sergienko,[2] Bahaa E. A. Saleh,[2] and Malvin C. Teich[1,2]

[1]Quantum Imaging Laboratory, Department of Physics, Boston University, 8 Saint Mary's Street, Boston, Massachusetts 02215

[2]Quantum Imaging Laboratory, Department of Electrical and Computer Engineering, Boston University, 8 Saint Mary's Street, Boston, Massachusetts 02215

(Received 8 April 1999)

We demonstrate the effective removal of intrinsic distinguishability between entangled-photon pairs in femtosecond spontaneous parametric down-conversion. High-visibility quantum interference is recovered (an increase to 96% from 17%) while preserving the high photon-flux density associated with the use of long nonlinear crystals. This new technique is expected to serve as a basic component in the preparation of multiphoton entangled states.

PACS numbers: 42.50.Dv, 03.67.–a, 42.65.Ky, 42.65.Re

The nonlinear-optical process of continuous-wave (cw) spontaneous parametric down-conversion [1] has long provided a useful source of nonclassical light for carrying out practical tests of the foundations of quantum mechanics. The nonlinear process takes place in a second-order nonlinear crystal pumped by a laser, and generates photon pairs in an entangled quantum state, as originally defined by Schrödinger [2]. Recent experiments with multiphoton entangled states in the areas of quantum teleportation [3,4], entanglement swapping [5], and tests of local realism (GHZ states) [6,7] have imposed an additional requirement—that independent photon pairs must be generated synchronously in different nonlinear crystals. To satisfy this requirement, ultrafast pump lasers (sub-psec regime) with pulse widths much shorter than the time of coherent nonlinear interaction in the crystal (which increases proportionally with crystal thickness) must be employed for the generation of multiphoton entangled states through parametric down-conversion. Unfortunately, however, quantum-interference experiments display strong decoherence effects [8,9] under these conditions.

None of the ultrafast type-II experiments reported thus far have exhibited visibility that is independent of crystal length, as a result of significant linear dispersion in the crystal arising from the different group velocities of the down-converted photons and the pump pulse. In spite of this, researchers have managed to obtain high-visibility fringes by using narrow-band interference filters placed before the detectors. This spectral *postselection* technique artificially increases the limited coherence time of the pairs produced by the brief pump pulses, and therefore restores the quantum interference to a degree. However, this benefit is accompanied by a drastic reduction of the photon-flux density reaching the detectors. The observation of multiphoton entangled states is greatly facilitated by a large photon-flux density.

In this Letter we demonstrate a new method which effectively removes the intrinsic distinguishability present in photon pairs generated via femtosecond down-conversion in long nonlinear crystals. This is achieved by drawing on the dual polarization and energy-time entanglement available in type-II optical parametric down-conversion [10]. While the rate of the photon-pair generation rate scales linearly with nonlinear crystal length, we demonstrate that the pattern of the measured coincidence rate is completely defined by the spectrum of the pump pulse and does not depend on the dispersion parameters of the crystal, nor on its length. The validity of our technique is experimentally demonstrated by the revival of high-visibility quantum interference (from 17% to 96%) in a photon-coincidence experiment *without the use of spectral filtering,* thereby preserving high photon-flux density at the detectors.

Cascaded transformations of the two-photon state.— Consider the quantum-interference experiment illustrated in Fig. 1. The two-photon state at the output of the β-barium borate (BBO) nonlinear down-conversion crystal is developed on the basis of one-dimensional (along the z axis) collinear type-II parametric down-conversion. The perturbed state (after evolution from initial time t_0 to time t) at the output of the nonlinear crystal of thickness L assumes a form that strongly depends on the region of *coherent* nonlinear interaction (d_{eff}) via the partial decoherence function $W(z-\xi)$, which is

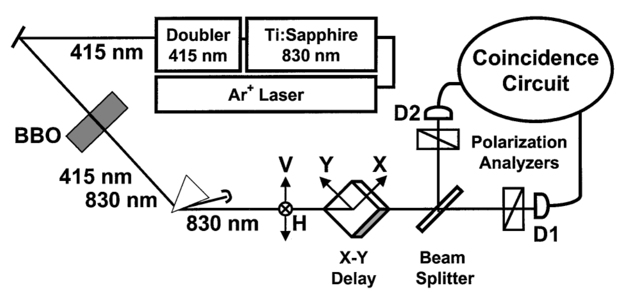

FIG. 1. Schematic of the polarization quantum-interference experimental setup.

 0031-9007/00/84(4)/618(4)$15.00

localized about an arbitrary position ξ in the nonlinear crystal [9]:

$$|\Psi_\xi^{(2)}\rangle \sim |0\rangle - \frac{i}{\hbar}\int_{t_0}^{t} dt'\,\chi^{(2)}\int_{-L}^{0} dz\, W(z-\xi) \times [E_p^{(+)}(t',z)\mathbf{e}_s\hat{E}_s^{(-)}(t',z)\mathbf{e}_i\hat{E}_i^{(-)}(t',z) + \text{H.c.}]|0\rangle. \tag{1}$$

Here $\chi^{(2)}$ is the second-order susceptibility of the nonlinear medium; $\mathbf{e}_j$ is the unit vector denoting the polarization state of the jth field $\hat{E}_j^{(-)}(t',z)$; the subscripts p, s, and i represent the pump, signal, and idler, respectively; the pump field is assumed to be a propagating classical transform-limited pulse whose amplitude is slowly varying:

$$E_p^{(+)}(t',z) = \sqrt{I_p\left(t' - \frac{z}{v_p}\right)}\exp[i(k_p^0 z - \omega_p^0 t')]. \tag{2}$$

The quantity $I_p(t',z)$ repeats the intensity profile of the pump at time t' and position z along the propagation axis with a full width at half maximum (FWHM) denoted τ_p. Because of the characteristic of our laser beam, we specifically chose it to have a Gaussian form, $\sqrt{I_p(t',z)} = \sqrt{I_0}\exp[-(t' - \frac{z}{v_p})^2/2\sigma^2]$ with $\sigma = \tau_p/(2\sqrt{\ln 2})$, though the theory is more general and can accommodate any pulse shape. The central wave number, carrier frequency, and group velocity of the pump (at the carrier frequency inside the nonlinear crystal) are denoted in Eq. (2) by k_p^0, ω_p^0, and v_p, respectively. The explicit form of $W(z-\xi)$ is taken to be a half-Gaussian with argument $(z-\xi)$ and width d_{eff}; its magnitude decreases with increasing argument as a consequence of the effective gradual separation of the pump pulse from the down-converted fields in the nonlinear crystal arising from linear dispersion. This function reflects the distinguishability not only between the down-converted photons of each pair but also between pairs born at different locations as the femtosecond pump pulse traverses the nonlinear crystal.

We now consider the timing diagram shown in Fig. 2 in conjunction with the schematic of our experimental apparatus presented in Fig. 1. Once an orthogonally polarized photon pair in the laboratory polarization basis [H (horizontal), V (vertical)] is generated at time t_0 around position ξ, it propagates through the nonlinear down-conversion crystal, acquiring a relative time delay ϕ_ξ imparted by the birefringence of the nonlinear crystal. The two-photon state in the (H,V) basis,

$$|\Psi_\xi^{(2)}\rangle \sim |V\rangle_{t_0}|H\rangle_{t_0+\phi_\xi}, \tag{3}$$

then propagates through a polarization delay line made of birefringent material (such as crystalline quartz) oriented so that its fast X (slow Y) axis is rotated by 45° with respect to the H (V) polarization axis (projection and optical-path-delay operations are displayed separately in

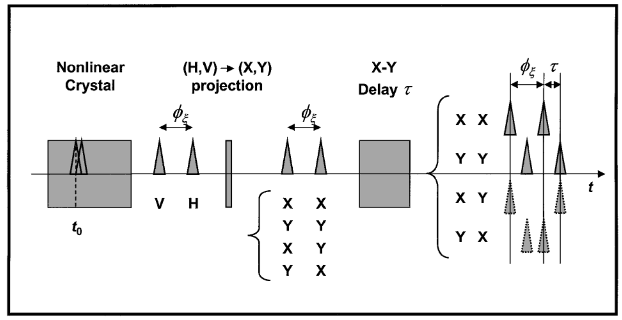

FIG. 2. A cross-polarized photon pair generated in the vicinity of position ξ within the nonlinear down-conversion crystal acquires a relative time delay ϕ_ξ. These photons are projected to a new basis (X,Y) that is tilted by 45° with respect to the original basis (H,V), and the Y-projected photon experiences a relative optical-path delay τ with respect to the X-projected photon as a result of the birefringence of the delay element. (Projection and optical-path delay operations are displayed separately for clarity.) Although there appear to be four possible configurations that the photon pair can assume before arriving at the beam splitter (far right), the bottom two (dotted) vanish because of their coefficients. The remaining two contributions (solid) preserve their *relative* delay ϕ_ξ, so that the interfering terms are the XX and YY terms with a delay τ, whatever the value of ϕ_ξ.

Fig. 2 for clarity). As a result of the projection, the two-photon state in the rectilinear (X,Y) basis becomes

$$|\Psi_\xi^{(2)}\rangle \sim (|X\rangle_{t_0} + |Y\rangle_{t_0})(|X\rangle_{t_0+\phi_\xi} - |Y\rangle_{t_0+\phi_\xi}). \tag{4}$$

Finally, the longitudinal optical-path delay τ along the Y axis with respect to the X axis gives rise to

$$|\Psi_\xi^{(2)}\rangle \sim (|X\rangle_{t_0}|X\rangle_{t_0+\phi_\xi} - |Y\rangle_{t_0+\tau}|Y\rangle_{t_0+\phi_\xi+\tau}) + (|Y\rangle_{t_0+\tau}|X\rangle_{t_0+\phi_\xi} - |X\rangle_{t_0}|Y\rangle_{t_0+\phi_\xi+\tau}), \tag{5}$$

which is illustrated at the far right of Fig. 2. This then arrives at a nonpolarizing beam splitter, as shown in Fig. 1, which injects photons into the two arms of the polarization interferometer (denoted in the following equations as subscripts 1 and 2). The polarization analyzers at the ends of the arms, being the final elements in the polarization interferometer, transform the two-photon state once more, via the operator $\hat{P} \equiv |\Theta\rangle_1|\Theta\rangle_2\,{}_2\langle\Theta|_1\langle\Theta|$, which is constructed in the polarization analyzer states Θ_1 and Θ_2.

Taking account of the transformations described above, one can calculate the two-photon detection probability amplitude

$$\mathcal{A}_\xi(t_1,t_2) = \langle 0|\hat{E}_1^{(+)}\hat{E}_2^{(+)}|\Psi_\xi^{(2)}\rangle, \tag{6}$$

where t_1 (t_2) denotes the event registration time at the detector located at the first (second) arm of the interferometer. For an arbitrary region about the position ξ in the crystal, Eq. (6) takes the explicit form [9]

$$A_\xi(T,t) \equiv \mathcal{A}_\xi(t_1,t_2) \sim \sqrt{I_p\left(T - \frac{\Lambda}{D}t - \frac{\xi}{v_p}\right)} \times W(t)\,\text{rect}_{[-L,0]}\left(\frac{t}{D} + \xi\right) \times \exp[i(k_p^0\xi - \omega_p^0 T)], \tag{7}$$

where $T = (t_1 + t_2)/2$, $t = (t_1 - t_2)$, $\Lambda = [1/v_p - (1/2)(1/v_s + 1/v_i)]$, and $D = (1/v_i - 1/v_s)$. The function $\mathrm{rect}_{[-L,0]}(z)$ has a unity value when its argument is in the range $[-L, 0]$ and vanishes otherwise, and $W(t)$ is the partial decoherence function discussed above.

When we carry out the above-described set of transformations, the rotated optical delay line causes multiple possibilities of coincidence detection, thereby yielding an overall two-photon detection probability amplitude that is the superposition of these possibilities. However, as a consequence of the cascaded transformations, the possibilities originating from the two right-most terms in Eq. (5) (shown as dotted in Fig. 2) vanish, leaving only two surviving terms that contribute to the overall two-photon amplitude:

$$B_{\xi,\tau}(T,t) \sim \cos\left(\frac{\pi}{4} - \theta_1\right)\cos\left(\frac{\pi}{4} - \theta_2\right)A_\xi(T,t) - \sin\left(\frac{\pi}{4} - \theta_1\right)\sin\left(\frac{\pi}{4} - \theta_2\right) \times A_\xi(T+\tau, t). \quad (8)$$

Finally, using Eq. (8) in the coincidence-count rate equation [1] provides

$$R(\tau) = \int_{-L+d_{\mathrm{eff}}}^{0} d\xi \int_{-\infty}^{\infty}\int_{-\infty}^{\infty} dT\, dt |B_{\xi,\tau}(T,t)|^2, \quad (9)$$

from which we determine the explicit form of the coincidence-count rate at the detectors, as a function of polarization-analyzer angles (θ_1, θ_2) and optical-path relative delay time (τ), to be

$$R(\theta_1,\theta_2,\tau) = G_p(0)\int_{-L+d_{\mathrm{eff}}}^{0} d\xi\, \Phi(\xi)\Big[(\cos^2\vartheta_1\cos^2\vartheta_2 + \sin^2\vartheta_1\sin^2\vartheta_2) - 2(\sin\vartheta_1\sin\vartheta_2\cos\vartheta_1\cos\vartheta_2)\frac{G_p(\tau)}{G_p(0)}\cos(\omega_p^0\tau)\Big], \quad (10)$$

where $G_p(\tau) = \int_{-\infty}^{\infty} dt \sqrt{I_p(t) I_p(t+\tau)}$ and $\vartheta_i \equiv \pi/4 - \theta_i$, $i = 1, 2$. All of the ξ-dependent terms in Eq. (10) are collected in the function $\Phi(\xi)$ so that the interference term (in square brackets) is generation-region independent. This reflects the successful liberation of entangled photon pairs from any influence of dispersion associated with the nonlinear crystal which results in the width of the quantum-interference pattern being solely determined by the pump-pulse duration τ_p.

Quantum-interference experiments with the new cascaded-transformation state.—Experiments were carried out using the experimental arrangement shown in Fig. 1. An actively mode-locked Ti:sapphire laser (pumped by a cw Ar-ion laser) emitted pulses of light at 830 nm. This radiation was frequency doubled to provide 80 fsec pulses (FWHM) at $\lambda_p = 415$ nm, with a repetition rate of 82 MHz and an average power of 15 mW.

This sequence of femtosecond pulses was delivered to a BBO crystal, where it underwent type-II spontaneous parametric down-conversion in a collinear degenerate ($\omega_1^0 = \omega_2^0 = \omega_p^0/2$) configuration. The collinear beam of down-converted photons was selected by a 2.5 mm circular aperture located about 7 cm beyond the crystal. After the residual pump pulses were separated from the signal and idler beams using a fused-silica dispersion prism, the down-converted photons were sent through the first stage of the cascaded-transformation apparatus which was composed of a birefringent material (crystalline quartz) whose fast axis was oriented at 45° with respect to the (H, V) laboratory coordinate system. Relative optical delay was introduced by changing the thickness of the birefringent material. The down-converted photons continued to a nonpolarizing beam splitter. The light at each output port of the beam splitter was then directed toward a Glan-Thompson polarization analyzer, and thence to a convex lens for focusing onto an actively quenched Peltier-cooled avalanche photodiode photon-counting detector. The detector event registrations were conveyed to a coincidence circuit with a 3 ns coincidence-time window. Corrections for accidental coincidences were not necessary.

Discussion.—The experimental data (solid squares) illustrated in the insets of Fig. 3 display the coincidence rates (CR) as a function of polarization-analyzer angle θ_2 when θ_1 is fixed at 0°. Coincidence patterns are shown for two representative relative optical-path delays: -96 fsec (left inset) and 0 fsec (right inset). The visibility of the coincidence pattern, $\mathcal{V} = (\mathrm{CR_{max}} - \mathrm{CR_{min}})/(\mathrm{CR_{max}} + \mathrm{CR_{min}})$, at 0 fsec delay turns out to be 96%, which is just a hair short of the theoretical maximum of 100%. This is to be compared with the rather anemic visibility of 17% that was observed in a similar configuration using a nonrotated polarization delay line [9] (time-delay fringes and polarization-rotation fringes are interchangeable, as has recently been established for femtosecond down-conversion [11]).

Coincidence patterns such as the representative ones shown in the insets were collected for various values of the relative optical-path delay τ. The open squares in the main plot of Fig. 3 represent the maximum and minimum values of the coincidence rate (connected by a vertical dashed line) for various values of τ. The coincidence-rate visibility is seen to decrease as τ deviates from 0 fsec. The width of the coincidence-rate pattern, which is about 80 fsec, is determined solely by the pump-pulse duration and demonstrates a crystal-dispersion-independent profile

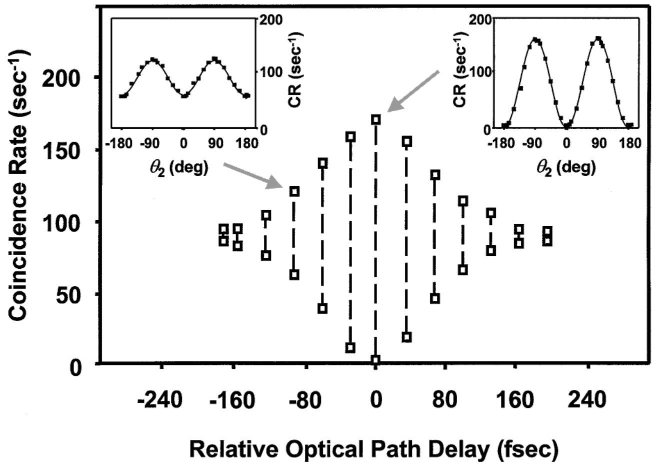

FIG. 3. Maxima and minima (open squares) of coincidence-rate quantum-interference patterns plotted as a function of relative optical-path delay time τ. Each pair of data points (connected by a dashed vertical line) corresponds to the maximum and minimum coincidence rates (CR, sec^{-1}) obtained from a polarization experiment at a particular value of τ (examples are shown in the insets) in which the angle θ_2 of the second polarization analyzer is varied while θ_1 is fixed at 0°. The visibility of the interference pattern is measured to be 96% at 0 fsec relative path delay and the width of the path-delay interference pattern nicely reveals the 80 fsec pump-pulse duration used in these experiments. This experiment was conducted using a 3 mm thick BBO crystal.

that remains identical for different thicknesses of the nonlinear down-conversion crystal.

To conclude, we have successfully co-opted the dual energy time and polarization entanglement inherent in type-II parametric down-conversion to implement a new scheme for eliminating the effects of decoherence in femtosecond parametric down-conversion. Despite our use of long nonlinear crystals, which permits high photon-flux densities to be obtained, we have obtained a high-visibility quantum-interference pattern without the use of spectral filtering. We expect that this new technique will find use in a range of quantum-optics applications.

We are grateful to Bradley M. Jost and Jan Peřina, Jr. for useful discussions. This work was supported by the National Science Foundation and the Boston University Photonics Center.

Note added in proof.—Since completing this work, a recently published paper [12] describing an experiment that achieves a visibility of 64% using a different technique has come to our attention.

[1] D. C. Burnham and D. L. Weinberg, Phys. Rev. Lett. **25**, 84 (1970); J. Peřina, Z. Hradil, and B. Jurčo, *Quantum Optics and Fundamentals of Physics* (Kluwer, Boston, 1994); L. Mandel and E. Wolf, *Optical Coherence and Quantum Optics* (Cambridge, New York, 1995), Chap. 22.

[2] E. Schrödinger, Naturwissenschaften **23**, 807 (1935); **23**, 823 (1935); **23**, 844 (1935) [translation in *Quantum Theory and Measurement,* edited by J. A. Wheeler and W. H. Zurek (Princeton University Press, Princeton, NJ, 1983)].

[3] C. H. Bennett, G. Brassard, C. Crépeau, R. Jozsa, A. Peres, and W. Wootters, Phys. Rev. Lett. **70**, 1895 (1993); D. Boschi, S. Branca, F. De Martini, L. Hardy, and S. Popescu, Phys. Rev. Lett. **80**, 1121 (1998).

[4] D. Bouwmeester, J.-W. Pan, K. Mattle, M. Eibl, H. Weinfurter, and A. Zeilinger, Nature (London) **390**, 575 (1997).

[5] J.-W. Pan, D. Bouwmeester, H. Weinfurter, and A. Zeilinger, Phys. Rev. Lett. **80**, 3891 (1998).

[6] D. M. Greenberger, M. A. Horne, and A. Zeilinger, in *Bell's Theorem, Quantum Theory and Conceptions of the Universe,* edited by M. Kafatos (Kluwer, Dordrecht, The Netherlands, 1989); D. M. Greenberger, M. A. Horne, A. Shimony, and A. Zeilinger, Am. J. Phys. **58**, 1131 (1990).

[7] D. Bouwmeester, J.-W. Pan, M. Daniell, H. Weinfurter, and A. Zeilinger, Phys. Rev. Lett. **82**, 1345 (1999).

[8] G. Di Giuseppe, L. Haiberger, F. De Martini, and A. V. Sergienko, Phys. Rev. A **56**, R21 (1997); W. P. Grice, R. Erdmann, I. A. Walmsley, and D. Branning, Phys. Rev. A **57**, R2289 (1998); W. P. Grice and I. A. Walmsley, Phys. Rev. A **56**, 1627 (1997); T. E. Keller and M. H. Rubin, Phys. Rev. A **56**, 1534 (1997); J. Peřina, Jr., A. V. Sergienko, B. M. Jost, B. E. A. Saleh, and M. C. Teich, Phys. Rev. A **59**, 2359 (1999).

[9] M. Atatüre, A. V. Sergienko, B. M. Jost, B. E. A. Saleh, and M. C. Teich, Phys. Rev. Lett. **83**, 1323 (1999).

[10] T. B. Pittman, Y. H. Shih, A. V. Sergienko, and M. H. Rubin, Phys. Rev. A **51**, 3495 (1995); Y. H. Shih and A. V. Sergienko, Phys. Lett. A **191**, 201 (1994).

[11] A. V. Sergienko, M. Atatüre, Z. Walton, G. Jaeger, B. E. A. Saleh, and M. C. Teich, Phys. Rev. A **60**, R2622 (1999).

[12] D. Branning, W. P. Grice, R. Erdmann, and I. A. Walmsley, Phys. Rev. Lett. **83**, 955 (1999).